



OPEN ACCESS

EDITED BY

Giacomo Montereale Gavazzi,
Royal Belgian Institute of Natural
Sciences, Belgium

REVIEWED BY

Evangelos Alevizos,
Université de Nantes, France
Lucia Margheritini,
Aalborg University, Denmark

*CORRESPONDENCE

Peter Feldens,
✉ peter.feldens@io-warnemuende.de

RECEIVED 31 January 2023

ACCEPTED 22 May 2023

PUBLISHED 08 June 2023

CITATION

Feldens A, Marx D, Herbst A, Darr A,
Papenmeier S, Hinz M, Zettler ML and
Feldens P (2023), Distribution of
boulders in coastal waters of Western
Pomerania, German Baltic Sea.
Front. Earth Sci. 11:1155765.
doi: 10.3389/feart.2023.1155765

COPYRIGHT

© 2023 Feldens, Marx, Herbst, Darr,
Papenmeier, Hinz, Zettler and Feldens.
This is an open-access article distributed
under the terms of the [Creative
Commons Attribution License \(CC BY\)](#).
The use, distribution or reproduction in
other forums is permitted, provided the
original author(s) and the copyright
owner(s) are credited and that the
original publication in this journal is
cited, in accordance with accepted
academic practice. No use, distribution
or reproduction is permitted which does
not comply with these terms.

Distribution of boulders in coastal waters of Western Pomerania, German Baltic Sea

Agata Feldens^{1,2}, Denise Marx¹, Anne Herbst^{1,3}, Alexander Darr¹,
Svenja Papenmeier¹, Matthias Hinz¹, Michael L. Zettler¹ and
Peter Feldens^{1*}

¹Leibniz Institute for Baltic Sea Research Warnemünde, Warnemünde, Germany, ²Subsea Europe Services GmbH, Rostock, Germany, ³University of Rostock, Faculty of Interdisciplinary Research, Department Maritime Systems, Rostock, Germany

This study contributes to a better understanding of geogenic reef distribution in the southern Baltic Sea and highlights the implications of survey-related factors on automated boulder classification when utilizing data from multiple surveys. The distribution of hard grounds and reefs is needed as a baseline for geological and biological studies, but also for offshore construction, navigation and coastal management. In this study we provide maps of the distribution of geogenic reefs for about 750 km² in the southern Baltic Sea, at the sites Wismar Bay, Darss Sill and Plantagenet Ground. The maps are based on full-coverage backscatter surveys with different side scan sonar and multibeam echo sounder systems. The distribution and number of boulders in the backscatter maps was determined using a convolutional neural network combined with quality control by human experts. The extent of the geogenic reefs was calculated on the basis of the number of boulders in 50 m x 50 m grid cells. We compare the results with previous reef maps based on point sampling, which show reefs of either biogenic or geogenic origin. According to the earlier maps, 11% of the Plantagenet Ground seabed was classified as reef habitat type. This is similar to the result of our study (12%), although we only considered reefs of geogenic origin. In the Darss Sill, geogenic reefs are larger in this study than in previous maps (30% versus 23%). In both regions, the spatial distribution of reefs differs significantly between old and new maps. For Wismar Bay, previous maps classify 3% of the seafloor as habitat type reef, whereas this study classifies 35% as geogenic reef. The use of automated classification during seafloor mapping allowed large areas to be interpreted in a few days. It also provided more information on the distribution of boulders within the geogenic reef. However, the boulder distribution maps show the negative effects of survey geometry, frequency and environmental conditions on automated boulder classification when data from different surveys are combined.

KEYWORDS

Baltic Sea, boulders, side scan sonar, backscatter, neural network, habitat mapping

1 Introduction

The morphological configuration and sediment composition of shallow continental shelf seas are influenced by various natural processes such as tides, waves, wind and sea level changes, but also by the regional geological history (Chiocci and Chivas, 2014).

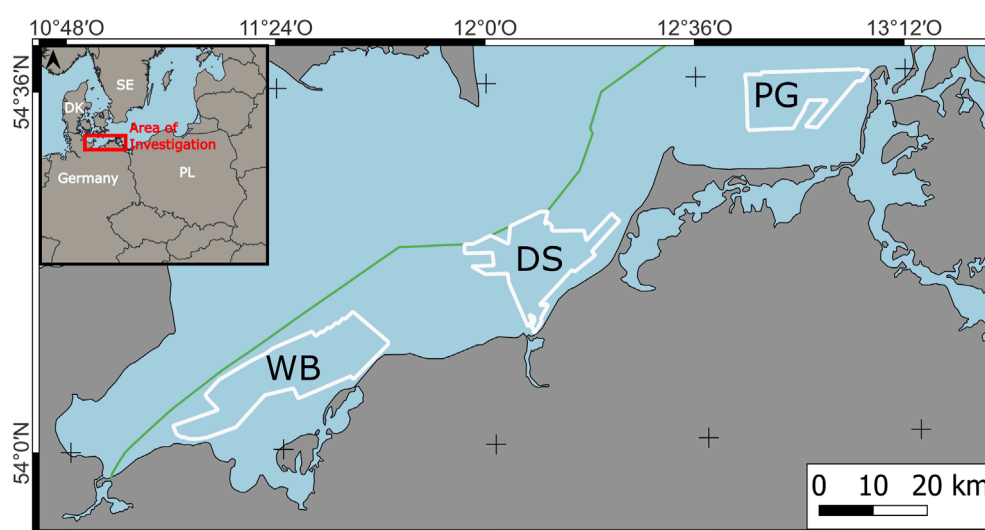


FIGURE 1

Location of the investigation sites in the southern Baltic Sea. WB, Wismar Bay. DS, Darss Sill. PTG, Plantagenet Ground.

Particularly in sediment-starved shelf seas—such as large parts of the Baltic Sea - the resulting patterns of mobile sediment and relict bedforms can be complex (Holland and Elmore, 2008). The composition of the seafloor is of geological interest and is also a key factor in understanding benthic habitats. Continental shelf seas are subject to a variety of anthropogenic impacts, such as mining, construction and tourism, and require management to balance different interests with environmental protection. Information on the composition of the seabed is also of key interest for this purpose. In addition to the distribution of clay, silt, sand and gravel sediments, and the distribution of organic material such as preserved peat and gyttja deposits, the distribution of ecologically valuable hard grounds needs to be known. In the southern Baltic Sea, hard grounds consists of cobbles (6.3–25.6 cm in diameter) and boulders (exceeding 25.6 cm in diameter), which may occur isolated or in clusters (Papenmeier et al., 2020). The cobbles and boulders erode from glacial till, deposited throughout the southern Baltic Sea during the last glaciations (Björck, 1995). In recent years, interest in the distribution of these hard grounds increased; both for identifying and understanding ecologically important (Beisiegel et al., 2019; Franz et al., 2021) habitats, but also to identify obstacles to offshore construction, e.g., of wind parks and related infrastructure such as cables. Chiefly due to their ecological value, the European Union implemented the protection of hard grounds in the European seas in 1992 (Papenmeier et al., 2020) as “geogenic reefs.” Reefs appear as distinctive morphological large-scale forms of the seafloor (Fink et al., 2017) and consist of biotope types with reef-typical biocoenoses (corresponding biotopes). In this context, a distinction is made between biogenic and geogenic reefs. Boulder clay ridges, block fields, residual sediments with stones and erratic blocks Boedeker and Heinicke. (2018) are examples of geogenic reefs in the Baltic Sea. Residual sediments are widespread in the Baltic Sea and are remnants of erosion of glacial till surfaces. In the Baltic Sea, prior studies operating with diver support and video camera observations highlighted the distribution of boulders and their impact on benthic

habitats in shallow waters (Franz et al., 2021; von Rönn et al., 2021). However, while providing results of high accuracy, the employed methodologies are unsuitable for large areas of interest. Basin-wide boulder detection relies on the manual interpretation of acoustic images (BSH, 2016; Heinicke et al., 2021). To automate the detection of individual boulders, convolutional neural networks (CNN) have been trained to detect boulder-sized and larger objects on the seafloor (Feldens et al., 2019; Michaelis et al., 2019; Feldens, 2020; Feldens et al., 2021; Steiniger et al., 2022). However, these models have not yet been applied to larger-scale investigation sites.

In this study, we apply these models to three study sites in the southern Baltic Sea to map the distribution of boulders in different regions by counting their number in 50 m × 50 m grid cells. The study examines the distribution of boulders at three sites - Outer Wismar Bay (WB), Darss Sill (DS) and Plantagenet Ground (PTG) - with a total covered area of 333 km², 246 km² and 174 km², respectively (Figure 1). Based on the distribution of boulders and residual sediment, we delineate the subtype “geogenic reef” of the habitat type “reef” (EU code 1170) according to the guidelines of Heinicke et al. (2021). We compare the results with previously published maps of the distribution of the habitat type “reef.” We discuss the distribution of boulders at these sites and highlight problems with automatically derived boulder density maps for larger sites and variable data quality.

2 Materials and methods

2.1 Acoustic data

To identify boulders, backscatter mosaics were recorded using a side scan sonar and, at one location in the Darss Sill, a multibeam echo sounder. Boulders are recognized by a typical texture in

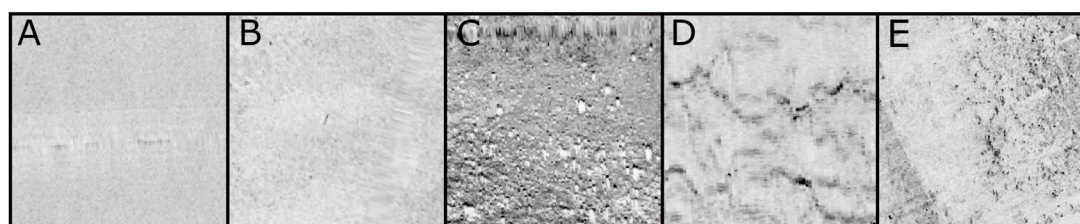


FIGURE 2

Examples of boulders occurrence in 50 m x 50 m SSS mosaic. (A) class 1, no boulder (B) class 2, 1 to 5 boulders (C) class 3, more than 5 boulders (D) effects of water column stratification. (E) effects of high mussel abundance.

backscatter mosaics, showing a high intensity side towards the side scan sonar, partially an intermediate backscatter surface, and an acoustic shadow forming at the far side of the boulder (examples are displayed in Figure 2). Side scan sonars and, for a smaller site, multibeam echo sounder with different frequencies (100–600 kHz) were available (Table 1). The processing of the side scan sonar data was done with the SonarWiz software, version 7, to apply geometric and radiometric corrections (Wilken et al., 2012). Corrections included bottom tracking and slant range correction, nadir filtering and an empirical gain normalization. The empirical gain normalization was done separately for each working area and each available frequency. R2Sonic multibeam echo sounder time series data was processed to backscatter mosaics with FMGT version 7.6. Exported Geo-TIFs with a resolution of 0.25 m served as the base for the following interpretation for sediment type (not reported in this study) and boulder presence. External government data, available as processed GeoTIFs at 0.25 m pixel resolution, was used where possible to reduce the survey time required.

2.2 Video data

Video stations were selected for ground truthing of hydroacoustic data. Video recordings were made at each station using a Sea Viewer SeaDrop 6000 HD for a minimum of 5 min. In addition, videos were taken along the transects at a speed of less than 1 knot for about 1 h. For the long video transects the Baltic Seafloor Imaging System (Beisiegel et al., 2017) was used.

2.3 Boulder distribution and reef maps

Boulders were detected semi-automatically using a workflow reported in Feldens et al. (2019). A neural network (YOLOv4 (Bochkovskiy et al., 2020)), detected individual boulders in the backscatter mosaics. The YOLOv4 model combines 29 convolutional layers with a total of 27.6 million parameters. The higher number of parameters allow to recognize features of different sizes within images. Input image resolution of the network is 512 × 512 pixels. The model uses the complete intersection of union (CIoU; Zheng et al. (2019)) as

TABLE 1 Overview of used side scan sonar and multibeam echo sounder systems. IOW, Leibniz Institute for Baltic Sea Research Warnemünde. BSH, Federal Maritime Agency. VBW, Vermessungsbüro Weigt.

| Side scan sonar | Frequency (kHz) | Source | Site |
|-------------------|-----------------|----------|-------------|
| Marine Klein 4000 | 100, 400 | IOW | DS, WB, PTG |
| Edgetech 4200 | 300, 600 | GeoGroup | DS |
| Edgetech 4300 MPX | 410 | BSH | DS, WB |
| Starfish 450F | 450 | IOW | DS |
| Edgetech 4200 HF | 300, 600 | VBW | DS, WB |
| R2Sonic2024 | 400 | IOW | DS |

the loss function, combined with DropBlock regularization (Ghiasi et al., 2018).

The trained Yolo-model generated for a previous study (Feldens et al., 2021) was reused for this task. The input to the model was the backscatter intensity in the form of 8-bit GeoTIFF mosaics. Grids derived from backscatter mosaics, such as texture metrics, were not computed as they are not expected to improve detection performance. While texture metrics can generally delineate rough substrates (Huvenne et al., 2002), they reduce the resolution of the input mosaics and are therefore detrimental to the individual detection of small objects. In the previous study, the model trained on side scan sonar backscatter mosaics achieved an accuracy of 43%, with a high number of false negatives in the detection of small boulders and false positives due to the effects of water column stratification observed in the outer parts of the side scan sonar swath range (Feldens et al., 2021). The model used 13,847 manually picked boulders and 2,349 blank examples as a training database. The training data was sliced into images of 64 × 64 pixels, with an overlap of 6 pixels. Images were enlarged to 512 × 512 pixels prior to training, and data augmentation by rotation, size and aspect was applied. In addition, image mosaicing of 4 separate training images to one mosaic for context independent training takes place. For model application, the mosaics of PTG, DS and WB were sliced into 64 × 64 pixel tiles, with a threshold of 0.2 for the intersection of the union value. Each tile took approximately 10 ms to process on an Nvidia 2080 TI graphics card. To visualise differences in boulder distribution within the geogenic reefs (Heinicke et al., 2021), boulder counts derived from the CNN were determined

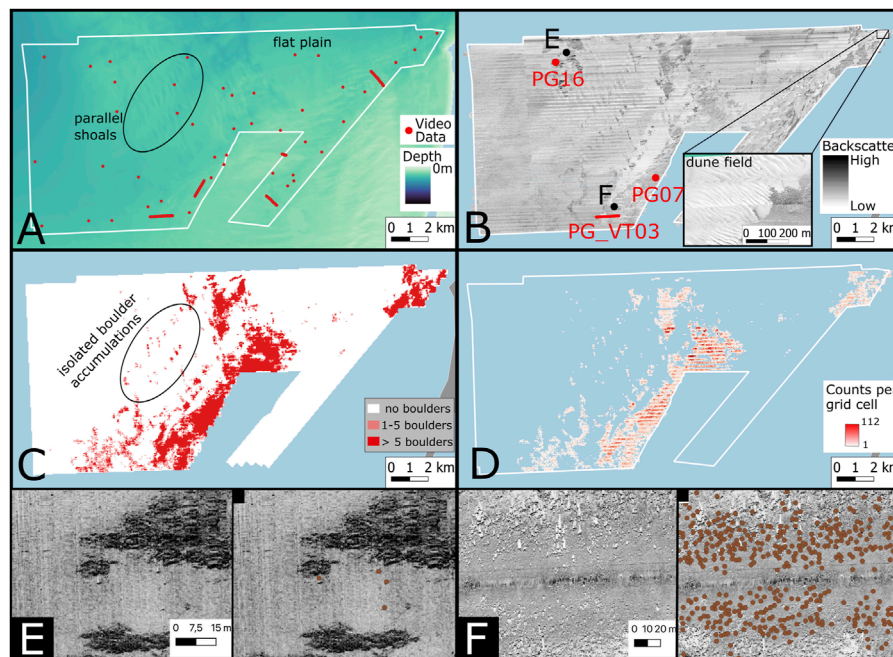


FIGURE 3

Results on the Plantagenet Ground. (A) Bathymetry (after Tauber, 2012) and video data available for validation of model output, (B) Side scan sonar backscatter mosaic, (C) Boulder class map (D) boulder counts per 50 m × 50 m grid cell, (E) high backscatter seafloor with few boulders, marked by dots, (F) variable across-track appearance and detection of boulders, marked by dots. A high number of false negative detections is present at high across-track distances.

TABLE 2 Boulder occurrence in the three focus sites.

| | WB | DS | PG |
|--------------|----|----|----|
| Class 1 (%) | 62 | 70 | 85 |
| Class 2 (%) | 8 | 13 | 5 |
| Class 3 (%) | 30 | 17 | 10 |
| Class -1 (%) | <1 | <1 | <1 |

per 50 m × 50 m grid. Partly, the same boulder can be detected several times by the neural network. To remove double detections, a buffer of 0.5 m (2 pixels) was placed around each detection. A dissolve operation merged overlapping buffers. For each remaining buffer, the centroid was calculated and used as the boulder position. All operations were done using QGIS 3.22.7.

Where possible, mosaics acquired at a frequency between 300 and 600 kHz were selected for boulder detection, as higher frequency mosaics showed better resolution of individual objects compared to mosaics acquired with sonars set to lower frequencies. The results were screened for false positives, taking into account available video profiles, and then divided into the three classes to generate a boulder distribution map according to the published guidelines for the identification of reefs (EU code 1170, subtype: geogenic reef) in German large-scale mapping surveys (Heinicke et al., 2021): Grid cells without blocks (class 1), cells

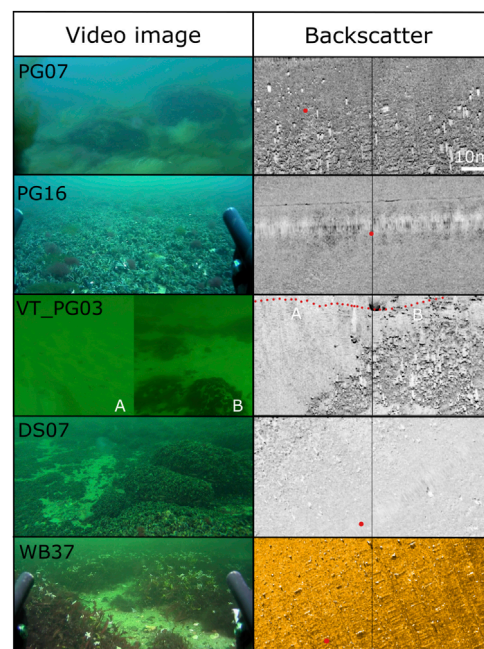


FIGURE 4

Examples of video images and the corresponding backscatter mosaics in two 50 × 50 m cells. The position of available video imagery is denoted by red dots.

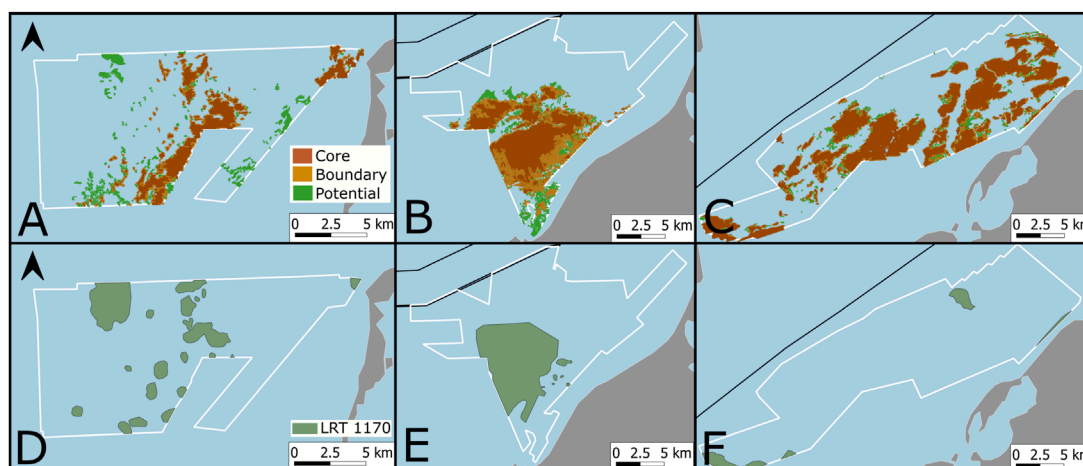


FIGURE 5

Comparison of reef classes identified in this study [(A), PTG, (B) DS, (C) WB] with published habitats of type reef [(D), PTG, (E) DS, (F) WB]. Source: IFAÖ (2005) and Wolf et al. (2011).

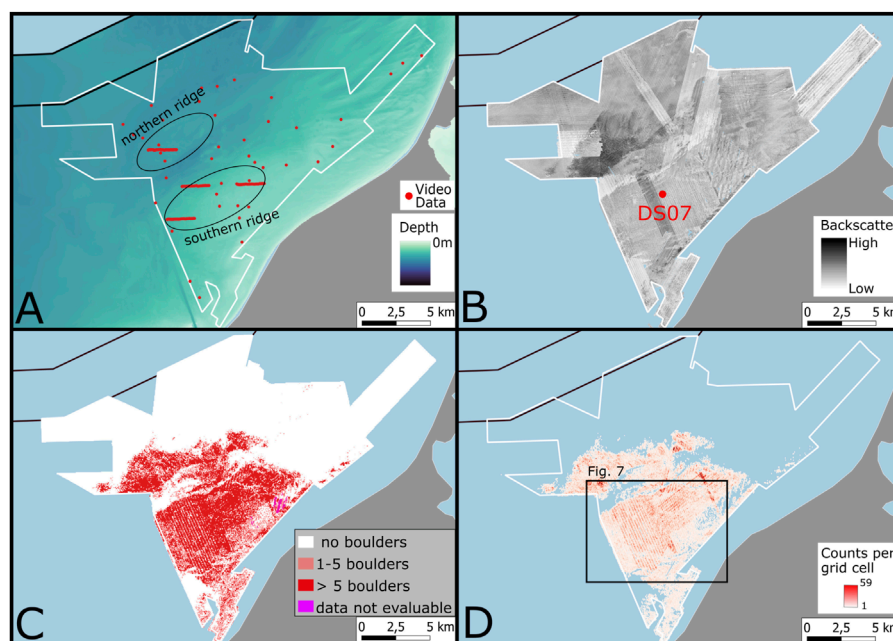


FIGURE 6

Results on the Darss Sill. (A) Bathymetry (Tauber, 2012) and video data available for validation of model output (B) Side scan sonar backscatter mosaic, (C) Boulder class map (D) boulder counts per 50 m × 50 m grid cell. The location of two ridges, separated by a channel, that host the majority of boulders in the DS area is indicated in (A).

with 1-5 blocks (class 2) and cells with more than 5 blocks (class 3). Example images of each class are shown in Figures 2A–C. In some cells, the quality of the backscatter mosaics did not allow a correct classification into class 1, 2 or 3. Where possible, the class was determined by the human interpreter during quality control based on the surrounding boulder distribution. Otherwise, the grid cells were identified as class –1. Poor data as well as false positive detections were caused by water column stratification,

which is common in the Baltic Sea and disturbs the hydroacoustic signal, or the presence of extensive mussel beds affecting the acoustic signal (Figures 2D, E). To map geogenic reef on large scales (Heinicke et al., 2021), published a mapping guide for using backscatter data with a resolution of 25 cm. Grid cells attributed to class 1–3 were used to produce maps of geogenic reefs, with the classification workflow explained in detail by Heinicke et al. (2021). Geogenic reefs are divided into core areas, boundary areas and

areas of potential reef occurrence (referred to as “development areas”). In simple terms, core reefs consist of areas larger than 1 ha with more than 5 boulders per 50 m × 50 m cell and more than 50% residual sediment. Boundary areas are adjacent to core reefs and are typically characterised by 1–5 boulders per cell and more than 50% residual sediment. The development areas are outside the core and boundary reefs and consist of areas larger than 1 ha with boulders or greater than 50% residual sediment.

3 Results

3.1 Plantagenet ground

The PTG is located north of the Fischland Darß-Zingst peninsula and west of the Isle of Hiddensee on the Rügen-Falster plateau in a water depth of 6–17 m in the photic zone. The investigated site covers 174 km² east of the Darss Sill. One third of the focus area (58 km²) is located in the national park “Vorpommersche Boddenlandschaft”, 56 km² in the Natura 2000 site “Plantagenet Ground” and 0.6 km² in the Natura 2000 site “Erweiterung Libben, Steilküste und Blockgründe Wittow und Arkona”. In the bathymetry (Tauber, 2012) and backscatter data (Figures 3A,B), parallel directed NE-SW running shoals occur in regular intervals in the central PTG. A mostly flat plain dominates the NE of the PTG. A dune field exists in the north-east and disappears with increasing depth.

The distribution of boulders in the PTG is shown in Figures 3C–E. Approximately 85% of the 50 m × 50 m grid was classified as class 1, less than 5% as class 2 and almost 10% as class 3 (Table 2). In this area class 3 is characterised by a very high density of boulders (Figure 4, PG07). The highest density of boulders occurs in the central NE-SW trending reef (Figure 3D). The area is also characterized by abrupt changes from sandy, boulder free areas to areas with a very high stone density (Figure 4, VT_PG03). The maximum number of counted boulders is 112 boulders (Figure 3F). Boulder density decreases towards the NE and W of PTG.

According to the guidelines for reef mapping and delineation (Heinicke et al., 2021), in the PTG about 9% of the total area belongs to the core reef, almost 3% to the boundary area and more than 4% to the development area (Figure 5A). A central boulder reef of more than 10 km² is oriented SW-NE. Its eastern part could not be mapped due to shallow water depths of less than 6 m. Additional boulder fields with a total area of 2.5 km² are observed close to the coast to the NE. Isolated NE-SW trending boulder accumulations, each less than 0.2 km², appear to be associated with the isolated high backscatter shoals where underlying glacial sediments crop out on the seafloor and form residual deposits. To the north-east of these isolated boulder reefs are two larger boulder reefs of almost 2 km². Notably, boulders do not occur in all areas of high backscatter, with no boulders observed in the far NW and E of PTG (Figure 3E). Here, the high backscatter is caused by the presence of mussels on the residual sediment (Figure 4, PG16).

3.2 Darss Sill

The DS is a submarine sill that separates the western part of the Baltic Sea from the central Baltic Sea (Figure 1 (Lemke et al., 1994)) and played a crucial role in the geological evolution of the Baltic Sea (Lemke and Kuijpers, 1995). The focus area covers 246 km². In the bathymetric data (Tauber, 2012), two till ridges rise in the West of the focus area and are separated by a channel incised by 21 m. Towards the east, this channel fades and the two ridges meet.

A methodological challenge on the DS is a very heterogeneous data set, collected with different sonar systems and data quality. The sensitivity of the automated detection system varies with data quality (especially the presence of water column stratification) and physical sonar parameters. Therefore, quantitative analysis of boulder abundance is more difficult compared to the other two focus sites with more homogeneous survey settings and instruments. Boulder occurrence is concentrated on the till ridges (Figures 6A,B). Towards the north boulders disappear with increasing water depth (Figure 6C). High mussel density affects the backscatter signal and degrades the data quality on the southern ridge, where a number of grid cells could not be interpreted (an example is shown in Figure 2).

Overall, 17% of the grids belong to class 3 (more than 5 boulders) and 13% to class 2 (1–5 boulders). No boulders were found in 70% of the grid cells. The maps showing counts per grid (Figure 6D) show localised areas of higher boulder density, particularly on the northern ridge. For the southern ridge, relative abundance assessments are influenced by mosaics of different frequencies (Figure 7). In addition to cross-track changes in boulder counts, the boundaries between different grids and instruments can be observed in the boulder count grids. Data recorded by the Edgetech 4200 (300 kHz) to the west of the DS show fewer boulders than adjacent data recorded by the Marine Klein 4000 sonar (400 kHz) and the Starfish 450F (450 kHz, Figure 6). It is noteworthy that in the latter system there is almost no cross-track variation in the number of boulders.

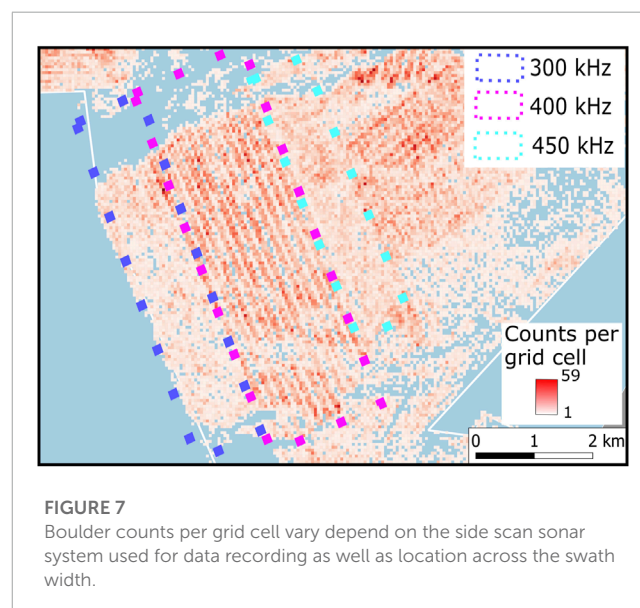


FIGURE 7
Boulder counts per grid cell vary depend on the side scan sonar system used for data recording as well as location across the swath width.

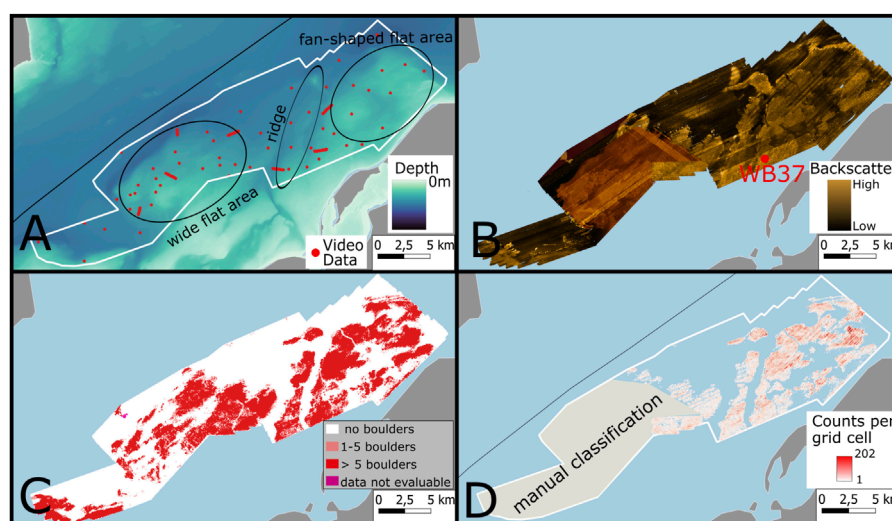


FIGURE 8

Results in Wismar Bay. Boulder detection by neural networks was only done for the eastern part of the investigation site, as the trained model was incapable of correctly interpreting externally provided mosaics (marked in D). (A) Bathymetry (Tauber, 2012) and video data available for validation of model output, (B) Side scan sonar backscatter mosaic, (C) Boulder class map (D) boulder counts per 50 m × 50 m grid cell.

According to the Heinicke et al. (2021) reef mapping guideline, almost 20% of the total area belong to the core reef class, less than 10% to the boundary reef class and about 5% to the development reef class (Figure 5B).

3.3 Outer Wismar Bay

The WB is located in the southern part of the Mecklenburg Bight 1. A total of 333 km² of hydroacoustic data in water depths from 12 m to 30 m have been collected during several cruises using side scan sonar, and external data provided by the authorities have been included for the interpretation of the boulder density (Figures 8A,B). The bathymetry shows three distinct elevations (Figure 8A). A broad area rises to depths of 10 m in the central WB and is separated from a northeast-southwest trending ridge by a channel up to 20 m deep. To the east, another channel separates the ridge from a broad fan-shaped area rising to 10 m depth.

The boulder distribution map could only be generated by CNN for the data recorded by the IOW (Figure 8C). Externally provided data was incompatible with the trained model, gave very poor performance and had to be manually edited. The NE-SW trending ridge and the fan-shaped shelf to the east are well represented by the boulder distribution map. Almost 30% of the grids are class 3 (more than 5 boulders) and more than 8% are class 2 (1–5 boulders). No boulders were detected on 62% of the area (Table 2). A map of counts per grid of individual neural network detections is shown in Figure 8D. The distribution of boulders reflects the morphological features of the WB, with higher densities in shallower waters and decreasing densities towards the basin. The maximum number of boulders detected is 202 per (50 x 50 m) grid cell. Dense clusters of boulders are particularly evident towards the east.

TABLE 3 Results of the comparison between the reef areas previously published and the reef classes identified in this study. The percentages of reefs within the focus areas were derived from digitized figures published in Wolf et al. (2011). To facilitate the comparison with published data, the classes ‘core reef’ and ‘boundary reef’ were merged and collectively referred to as ‘reef’. Similarly, the class “development area” was combined with the class “no reef”.

| | PG area (%) | DS area (%) | WB area (%) |
|----------------------|-------------|-------------|-------------|
| This study | | | |
| Reef | 12.1 | 29.6 | 35.2 |
| No reef | 87.9 | 70.5 | 64.8 |
| LRT published | | | |
| Reef | 10.99 | 22.70 | 2.79 |
| No reef | 89.01 | 77.30 | 97.21 |

In the WB, more than 31% of the area belong to the core reef, more than 4% to the boundary reef and about 2% to the development area (Figure 5C).

3.4 Comparison with available data

The State Office for the Environment, Nature Conservation and Geology publishes designated and nationally and internationally reported areas of the marine natural habitat type “reef” (EU HD, code 1170) in the coastal waters of Western Pomerania (Figures 5 D–F). A comparison between the spatial distribution of the published reef delineations and the geogenic reef areas mapped according to the workflow of Heinicke et al. (2021) shows a considerable discrepancy in abundance, spatial distribution or both (Figure 5; Table 3).

On PTG, the area percentages between the acoustic survey and the habitat type reef maps are comparable, with about 12% of the combined core and boundary reefs (corresponding to the habitat type “reef”) in this study compared to about 11% based on the published habitat maps. However, the geogenic core reef in the far northeast of PTG is severely underestimated in terms of area. Development areas in the east with high mussel densities and residual sediments are not identified as reefs in the published maps. In general, development areas are still subject to the establishment of criteria for recognition as reef areas through biological verification of residual sediment as a reef-building substrate (Heinicke et al., 2021). In the northwest, the published reef maps indicate an area of 19 km², but we could not locate any boulders in the acoustic data. The backscatter data in this area were characterised by patches of high backscatter intensity. The underwater video shows a dense mussel cover with some bare residual sediment located at the high backscatter patches and could be a potential biogenic reef, as described for the German exclusive economic zone (Boedeker and Heinicke, 2018).

In the DS, the sum of core and boundary reefs identified from the acoustic survey is approximately 30% after applying the mapping guideline (Heinicke et al., 2021). Approximately 23% of the DS was previously identified and designated as reefs. For the DS, the spatial match between the published maps and the detected boulder distribution is good, although the boulder-free channel between the two ridges is not shown on the published map. Based on the acoustic survey, the reef extends further to the southwest, explaining the difference in area percentage.

A major difference between the published reef maps and the geogenic reef mapping of this study is recognised for the WB. In contrast to the other focus areas, the distribution of designated reefs and identified core, boundary and potential reef areas differs significantly. Approximately 35% of the core and boundary reef areas in this study were identified using hydroacoustic data. Less than 3% of the reef area in the WB has been previously identified. The boulder accumulations that occur near the shallows in the centre of the WB, the NW-SE trending ridge and the fan-shaped elevations were previously missed. The central reef platform, identified by the hydroacoustic survey as the core reef, is largely missing from published reef maps.

4 Discussion and conclusion

The guidelines for preparation of geogenic reef classes (Heinicke et al., 2021) were found to be suitable for larger-scale application. The guidelines successfully account for the variable across-track sensitivity of the side-scan sonar mosaics with respect to boulder detection. An example illustrating this phenomenon is presented in Figure 3F. The resulting distribution of reefs into three classes is also not visibly affected by the frequency-specific boulder detection observed in the DS (Figure 6), allowing data from different side scan sonar systems and surveys to be combined. However, this robustness of the guideline Heinicke et al. (2021) to artefacts and sonar parameters is derived from not fully exploiting the information content of the backscatter mosaics. The maximum of 5 boulders in 50 m × 50 m cells (originally chosen because of the feasibility of manual classification) is low, as the maximum observed

number of boulders counted by the neural network in this study can exceed 200. Maps of boulder count allow to further subdivide the core reefs to areas of different boulder abundance. As the structure of the benthic community depends (among other factors) on the distribution of boulders (Franz et al., 2021), taking into account the variability of rock abundance would improve the understanding of ecosystem functions. The current threshold of five boulders for the core reef class is even more limiting when considering that previous studies have reported that at 0.2 m backscatter mosaic resolution, hard ground settlement space is underestimated by 42% (von Rönn et al., 2019), with underwater video imaging required to obtain a complete picture of the distribution of cobbles and boulders (Franz et al., 2021). Therefore, the amount of boulders identified in this study will be severely underestimated due to the 25 cm resolution of side scan sonar mosaics used in this study, combined with the workflow to remove double detections that is also sensitive to different boulders located in close vicinity. Therefore, the boulder numbers reported in this study should be taken as a minimum value. This situation may improve as synthetic aperture sonar surveys (Hayes and Gough, 2009) become more widely available, increasing resolution to the centimetre scale. Further underestimation of the number of counted boulders occurs for small boulders represented by few pixels, where detection performance drops off sharply for objects represented by only a few pixels (Ren et al., 2018; Feldens, 2020).

Camera observations and diving are only feasible for small survey areas or under suitable conditions (including water depth, weather and wind conditions). It is important to note that a 50 × 50 m cell cannot be validated using video alone. The video transect plot depicted in Figure 4 VT_PG03, serves as an illustration of how classifying a cell based on video imagery alone can lead to misinterpretation. In the provided example, the left cell, despite appearing devoid of boulders (class 1) in the video data, actually belongs to class 3 due to the evident accumulation of boulders in the southeast, as observed in the acoustic mosaic. Acoustic surveys are required to map reef structures over larger areas. In the coastal waters of Western-Pomerania considered in this study, the available reef maps are not based on targeted mapping of areas of marine habitat types (Figure 5). Reef areas were determined by point surveys or modelled habitat distribution and therefore correspond to an estimated polygon rather than an actual mapped area. Various data sources (e.g., grab sample protocols, underwater video footage) were collected, evaluated and interpreted for the previously available maps. Therefore, there can be large differences between the published distribution of the habitat type reef and the actual conditions on the seafloor (Figure 5 and summarised in Table 3), both in the location of reefs and in the percentage of area covered. The inadequate data set is likely to have implications for maritime spatial planning, and it is strongly recommended that the remaining parts of the coastal waters of Western-Vorpommern - and other regions - be validated for the presence of reefs through targeted surveys.

However, further development of automated boulder detection is required. In particular, the DS boulder map demonstrates the higher data homogeneity requirements needed for boulder abundance maps (Figure 7). Parameters such as survey geometry (especially angle of incidence), resolution (especially along track resolution, which is limited by vessel speed) and sonar parameters

(especially frequency and pulse length) cannot be corrected in post-processing. Hence, the inter-survey comparability of boulder distribution maps will remain limited due to discrepancies in the frequency and beamwidth of different systems, resulting in variations in physical resolution (Lurton, 2002). **Figure 7** demonstrates the disparities in boulder abundance attributed to frequency differences. On the other hand, inter-survey backscatter variations associated with uncalibrated backscatter data and artifacts like stripe noise can be rectified (Misiuk et al., 2020) (Wilken et al., 2012). However, it should be noted that these parameters do not impact the performance of the neural network. The mean backscatter intensity of the model's 64 x 64 input tiles does not influence the results, and stripe noise, such as nadir lines, is not misclassified by the model (Feldens et al., 2021). It is therefore recommended that surveys for boulder detection are carried out with constant frequency, pulse length and ship speed as well as limited swath width in order to keep the resolution as constant as possible. Finally, the improvement of neural network models applied to sonar data (Steiniger et al., 2022) improving the still low performance of the boulder detection models and a broader training database will also affect the results of boulder density surveys. Given the automated process and rapid interpretation of mosaics by neural networks (less than a day of computation time for the area considered in this study), data can be reprocessed using new models without undue effort.

In addition to the local abundance of boulders, the size distribution of boulders was found to influence the composition of benthic communities (Franz et al., 2021). The CNN used in this study only detects objects. In principle, the individual boulders could be segmented to calculate boulder size (Steiniger et al., 2022). However, the use of side scan sonar images is not sufficient for this task: no information on the vertical extent is preserved in the backscatter mosaics due to the removal of the water column during data processing (Blondel, 2010). In addition, the characteristic feature of the boulders on which the models are trained is the presence of an acoustic shadow. The shadow extension for a boulder of a given height depends on the slant range and the sonar height above the seafloor (Papenmeier et al., 2020). Boulders smaller than the spatial resolution of a grid cell can increase local backscatter. For these reasons, there is no clear relationship between boulder size and appearance in backscatter mosaics, and it is unlikely to exist given the additional effects of boulder shape, seasonality and epibenthic communities on the backscatter signal. Side scan sonar mosaics can only provide a first approximation of boulder size. Therefore, segmentation of multibeam echo sounder point cloud data with the maximum amount of preserved vertical information may be promising for future work on core reef boulder variability in the shallow coastal waters considered here.

Data availability statement

The raw data supporting the conclusion of this article will be made available by the authors, without undue reservation. Maps of boulder distribution and sediment distribution have been submitted to <https://www.geoseaportal.de/>, maintained by the Bundesamt für Seeschifffahrt und Hydrographie (BSH).

Author contributions

PF and AF conceived the study. MZ led the ATLAS project. AF and PF did the acoustic surveys. AF, PF, SP, DM, AH, AD, and MH contributed to data processing and data interpretation. DM, AH and AD did ground truthing by camera observations. AF and PF wrote the original draft. DM, AH, AD, SP, MH, and MZ edited the draft. All authors contributed to the article and approved the submitted version.

Funding

The project “Kartierung der Lebensräume (Biotop) und deren Lebensgemeinschaften am Meeresboden in den Küstengewässern Mecklenburg-Vorpommerns” was funded by the “Landesamt für Umwelt, Naturschutz und Geologie Mecklenburg-Vorpommern”, grant number 220-01-Sc-19.

Acknowledgments

We thank the captain and crew of the RV Elisabeth Mann Borgese for their assistance during our surveys. We would like to acknowledge the fruitful cooperation with the authorities of Vorpommern during the ATLAS project, especially with Mario von Weber. We would also like to thank Paul Nolte, who built a ModelBuilder for ArcGIS as part of his bachelor thesis, which was used to check and correct the individual steps of the reef mapping instructions, as well as Tim Bildstein (BioConsult GmbH & Co. KG.) and Kathrin Heinicke (Federal Nature Conservation Agency), who controlled the ModelBuilder. We would also like to thank the surveying company Vermessungsbüro Weigt and the “Staatliches Amt für Landwirtschaft und Umwelt Mittleres Mecklenburg (StALU-MM)” for providing the external data.

Conflict of interest

The authors declare that the research was conducted in the absence of any commercial or financial relationships that could be construed as a potential conflict of interest.

Publisher's note

All claims expressed in this article are solely those of the authors and do not necessarily represent those of their affiliated organizations, or those of the publisher, the editors and the reviewers. Any product that may be evaluated in this article, or claim that may be made by its manufacturer, is not guaranteed or endorsed by the publisher.

References

- Beisiegel, K., Darr, A., Gogina, M., and Zettler, M. L. (2017). Benefits and shortcomings of non-destructive benthic imagery for monitoring hard-bottom habitats. *Mar. Poll. Bull.* 121, 5–15. doi:10.1016/j.marpolbul.2017.04.009
- Beisiegel, K., Tauber, F., Gogina, M., Zettler, M. L., and Darr, A. (2019). The potential exceptional role of a small baltic boulder reef as a solitary habitat in a sea of mud. *Aquatic Conservation Mar. Freshw. Ecosyst.* 29, 321–328. doi:10.1002/aqc.2994
- Björck, S. (1995). A review of the history of the baltic sea, 13.0-8.0 ka bp. *Quat. Int.* 27, 19–40. doi:10.1016/1040-6182(94)00057-c
- Blondel, P. (2010). *The handbook of sidescan sonar*. Springer Science & Business Media.
- Bochkovskiy, A., Wang, C. Y., and Liao, H. Y. M. (2020). Yolov4: Optimal speed and accuracy of object detection. arXiv 2004.
- Boedeker, D., and Heinicke, K. (2018). *BfN-Kartieranleitung für "Riffe" in der deutschen ausschließlichen Wirtschaftszone (AWZ)*. Federal Agency for Nature Conservation, Germany, Vilm.
- BSH (2016). *Guideline for seafloor mapping in German marine waters using high-resolution sonars*. BSH, 147.
- Chiocci, F. L., and Chivas, A. R. (2014). Chapter 1 an overview of the continental shelves of the world. *Geol. Soc. Lond. Memoirs* 41, 1–5. doi:10.1144/m41.1
- Feldens, P., Darr, A., Feldens, A., and Tauber, F. (2019). Detection of boulders in side scan sonar mosaics by a neural network. *Geosciences* 9, 159. doi:10.3390/geosciences9040159
- Feldens, P. (2020). Super resolution by deep learning improves boulder detection in side scan sonar backscatter mosaics. *Remote Sens.* 12, 2284. doi:10.3390/rs12142284
- Feldens, P., Westfeld, P., Valerius, J., Feldens, A., and Papenmeier, S. (2021). Automatic detection of boulders by neural networks: A comparison of multibeam echo sounder and side-scan sonar performance. *J. Appl. Hydrogr.* 119, 6–17.
- Fink, P., Heinze, S., Raths, U., Riecken, U., and Ssymank, A. (2017). Rote liste der gefährdeten biotoptypen deutschlands (dritte fortgeschriebene fassung). *Naturschutz Biol. Vielfalt.undesamt für Naturschutz Bonn* 156, 460.
- Franz, M., von Rönn, G. A., Barboza, F. R., Karez, R., Reimers, H. C., Schwarzer, K., et al. (2021). How do geological structure and biological diversity relate? Benthic communities in boulder fields of the southwestern Baltic Sea. *Estuaries Coasts* 44, 1994–2009. doi:10.1007/s12237-020-00877-z
- Ghiasi, G., Lin, T. Y., and Le, Q. V. (2018). "Dropblock: A regularization method for convolutional networks," in *Advances in neural information processing systems*. Editors S. Bengio, H. Wallach, H. Larochelle, K. Grauman, N. Cesa-Bianchi, and R. Garnett (Curran Associates, Inc.).
- Hayes, M. P., and Gough, P. T. (2009). Synthetic aperture sonar: A review of current status. *IEEE J. Ocean. Eng.* 34, 207–224. doi:10.1109/joe.2009.2020853
- Heinicke, K., Bildstein, T., Boedeker, D., Schuchardt, B., Reimers, H. C., Heinrich, C., et al. (2021). *Leitfaden zur großflächigen Abgrenzung und Kartierung des Lebensraumtyps "Riffe" in der deutschen Ostsee (EU Code 1170; Untertyp: Geogene Riffe)*. Federal Agency for Nature Conservation, Germany, Vilm.
- Holland, K., and Elmore, P. (2008). A review of heterogeneous sediments in coastal environments. *Earth-Science Rev.* 89, 116–134. doi:10.1016/j.earscirev.2008.03.003
- Huvenne, V., Blondel, P., and Henriot, J. P. (2002). Textural analyses of sidescan sonar imagery from two mound provinces in the porcupine seabight. *Mar. Geol.* 189 (3-4), 323–341. doi:10.1016/s0025-3227(02)00420-6
- IfAÖ (2005). *Marine habitat types according to the EU Habitats Directive in the Mecklenburg-Western Pomerania area of the Baltic Sea*. Unpublished report on behalf of the Landesamt für Umwelt, Naturschutz und Geologie MV, Güstrow [in German].
- Lemke, W., Kuijpers, A., Hoffmann, G., Milkert, D., and Atzler, R. (1994). The darss sill, hydrographic threshold in the southwestern baltic: Late quaternary geology and recent sediment dynamics. *Cont. Shelf Res.* 14, 847–870. doi:10.1016/0278-4343(94)90076-0
- Lemke, W., and Kuijpers, A. (1995). Late pleistocene and early holocene paleogeography of the darss sill area, southwestern baltic. *Quat. Int.* 27, 73–81. doi:10.1016/1040-6182(94)00063-b
- Lurton, X. (2002). *An introduction to underwater acoustics: Principles and applications*. Springer Science & Business Media.
- Michaelis, R., Hass, H. C., Papenmeier, S., and Wiltshire, K. H. (2019). Automated stone detection on side-scan sonar mosaics using haar-like features. *Geosciences* 9, 216. doi:10.3390/geosciences9050216
- Misiuk, B., Brown, C. J., Robert, K., and Lacharité, M. (2020). Harmonizing multi-source sonar backscatter datasets for seabed mapping using bulk shift approaches. *Remote Sens.* 12, 601. doi:10.3390/rs12040601
- Papenmeier, S., Darr, A., Feldens, P., and Michaelis, R. (2020). Hydroacoustic mapping of geogenic hard substrates: Challenges and review of German approaches. *Geosciences* 10, 100. doi:10.3390/geosciences10030100
- Ren, Y., Zhu, C., and Xiao, S. (2018). Small object detection in optical remote sensing images via modified faster r-cnn. *Appl. Sci.* 8, 813. doi:10.3390/app8050813
- Steiniger, Y., Kraus, D., and Meisen, T. (2022). Survey on deep learning based computer vision for sonar imagery. *Eng. Appl. Artif. Intell.* 114, 105157. doi:10.1016/j.engappai.2022.105157
- Tauber, F. (2012). Meeresbodensedimente und meeresbodenrelief in der deutschen ostsee: Datenpositionen und blattschnitt, karte nr 2930 = seabed sediments and seabed relief in the German baltic sea: Data positions and sheet index. map no.2930 [map] 1 : 550 000, 54°n.
- von Rönn, G. A., Krämer, K., Franz, M., Schwarzer, K., Reimers, H. C., and Winter, C. (2021). Dynamics of stone habitats in coastal waters of the southwestern baltic sea (hohwacht bay). *Geosciences* 11, 171. doi:10.3390/geosciences11040171
- von Rönn, G. A., Schwarzer, K., Reimers, H. C., and Winter, C. (2019). Limitations of boulder detection in shallow water habitats using high-resolution sidescan sonar images. *Geosciences* 9, 390. doi:10.3390/geosciences9090390
- Wilken, D., Feldens, P., Wunderlich, T., and Heinrich, C. (2012). Application of 2d Fourier filtering for elimination of stripe noise in side-scan sonar mosaics. *Geo-Marine Lett.* 32, 337–347. doi:10.1007/s00367-012-0293-z
- Wolf, F., Gosselck, F., Bönsch, R., Hoth, T., and Gebhardt-Jesse, U. (2011). Bericht 1170 Riffe. Bericht des IfAÖ für das Landesamt für Umwelt, Naturschutz und Geologie MV, Güstrow. Available At: https://www.lung.mv-regierung.de/dateien/ffh_sb_irt_1170.pdf.
- Zheng, Z., Wang, P., Liu, W., Li, J., Ye, R., and Ren, D. (2019). Distance-iou loss: Faster and better learning for bounding box regression. ARXIV. doi:10.48550/ARXIV.1911.08287